Proc. NIPR Symp. Upper Atmos. Phys., 1, 173-184, 1988

SOME CHARACTERISTICS AND PROPAGATION OF WHISTLER-MODE LF/MF EMISSIONS AS OBSERVED AT LOW ALTITUDES ABOVE THE ANTARCTIC REGION WITH ISIS-1

Kazuhiro AIKYO*, Tadanori ONDOH and Kazuhiro OHTAKA

Radio Research Laboratory, 2-1, Nukui-Kitamachi 4-chome, Koganei-shi, Tokyo 184

Abstract: The broadband whistler-mode (w-mode) emissions in LF/MF bands observed at low altitudes in the nighttime auroral zone are examined in detail, especially from the viewpoint of the spectral characteristics and directions of wave vectors of the emissions using the ISIS-1 data including the fixed and swept frequency ionograms and AGC voltage traces of the sounder receiver. The emissions are characterized by spectra with relatively sharp upper cutoff ranging 0.75 to $0.4f_H$ (f_H: electron gyrofrequency) and with lower frequency cutoff less than 0.1 MHz (the lowest frequency of the sounder) for many cases. The directions of wave vectors at the satellite are determined from the antenna orientation at the instant when the emissions exhibit intensity minima on AGC voltage traces in the fixed frequency mode. The resultant directions of wave vectors are used as initial conditions for ray tracing to locate the source regions and to know the directions of wave vectors at the source region. It is shown that the cyclotron maser instability driven by auroral electron with upward loss cone at low altitudes is the most probable source mechanism which explains some characteristics of the observed emissions, particularly, of their high frequency portion.

1. Introduction

At Syowa Station, Antarctica, a telemetry reception of ISIS satellite data has continued since April 1976 in addition to various kinds of aeronomical observations. The topside sounding observations with swept and fixed frequency modes provide valuable information on a variety of auroral zone radio emissions in low (LF) and medium frequency (MF) bands. The radio noise data are obtained by monitoring the AGC voltages of the sounder receiver, and ambient plasma parameters scaled from conventional topside ionograms enable us to identify the propagation modes of received emissions. A preliminary analysis of ISIS-1 data acquired at Syowa Station has revealed AKR activities in the dayside cusp region as well as nightside auroral zone (AIKYO *et al.*, 1982).

Among various types of nightside auroral emissions in LF/MF bands observed by rockets and satellites, the whistler-mode (w-mode) emissions have been examined most elaborately. Since the report of preliminary results of ISIS-1 on w-mode emis-

* Present address: Kimitsu Satellite Control Center, Telecommunications Satellite Corporation of Japan, Sasa, Kimitsu-shi 292-05.

sions (MULDREW, 1970), statistical studies were made of occurrence and intensity pattern of the emissions for wide frequency range including LF/MF bands using Alouette 2 data (BARRINGTON *et al.*, 1971). Furthermore, w-mode emissions in LF/MF in the dayside cusp were studied in connection with soft electron precipitation (JAMES, 1973).

The banded w-mode emissions in LF/MF bands were observed by a rocket experiment in Antarctica and discussed in association with wave-particle interactions using simultaneous observations of the flux of precipitating electrons (OYA *et al.*, 1980). The auroral LF hiss with steady dynamic spectrum was also observed at low altitudes by Ohzora satellite (MORIOKA and OYA, 1985).

The studies of auroral radio emissions including w-mode emissions were made comprehensively with emphasis on the propagation modes depending on the ambient plasma parameters, and a cyclotron maser instability was concluded to be their generation mechanism after analyzing the high altitude data (BENSON, 1985) and low altitude data (BENSON and WONG, 1987) of ISIS-1.

This report presents briefly some characteristics of relatively intense w-mode emissions observed at low altitudes near the perigee of ISIS-1 where the plasma frequency f_N is greater than the electron gyrofrequency f_H, and the direction of arrival of the emissions at receiving antenna for a specified event, derived from spin-modulated signal intensity data with fixed frequency. Ray tracing is made to locate the source region using the observed directions as the initial condition, and a possible generation mechanism is discussed on the basis of spectral and propagation characteristics.

2. Observations

2.1. Spectral characteristics

The w-mode emission events are selected from the ISIS-1 sounder data obtained by telemetry reception at Syowa Station, Antarctica from April 1976 to December 1981. Low altitudes (lower than 1000 km) and nighttime (1700–0400 MLT) are the criteria to choose data for the present analysis. Additional condition is tentatively imposed that the sounder fixed frequencies must be either of the lowest two frequencies, 0.25 and 0.48 MHz, since these frequencies could cover w-mode emissions seen on the ionograms as well as AGC voltage traces, enabling us to determine the wave vector direction of the emissions with the help of antenna orientation derived from the magnetometer data. The passes which meet these conditions are the followings;

(1) November 16, 1977, 0020–0032 UT (0320–2047 MLT)
(2) November 14, 1978, 2220–2225 UT (2355–1947 MLT)
(3) November 15, 1978, 2152–2158 UT (2304–1750 MLT)
(4) October 29, 1979, 2059–2102 UT (2326–2257 MLT).

The first three passes cover the perigee ($\sim$600 km), and the last one covers the altitudes from 940 to 800 km. The emissions can be seen on thirty three ionograms acquired on these four passes.

Figure 1 shows a representative example of w-mode emissions observed near the perigee in the ionograms with fixed (0.48 MHz) and swept frequency mode. In the fixed frequency record the emissions exhibit a typical spin-modulated pattern and

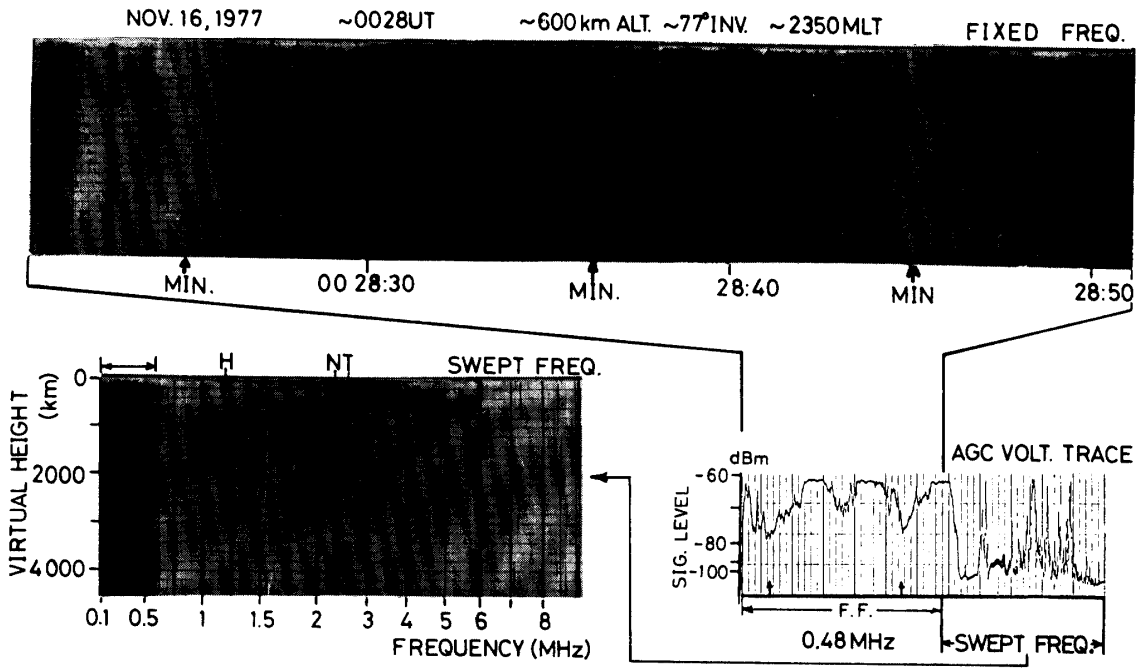

Fig. 1. Typical example of auroral whistler-mode emissions (hiss) in LF/MF bands as seen on the AGC voltage trace, fixed (F.F.) and swept frequency ionograms obtained near ISIS-1 perigee (~600 km). The arrows labelled by "MIN" indicate the time when the intensity minima occur as estimated from AGC data. Alphabetical letters, H, N and T stand for local electron gyro-, plasma and upper hybrid resonance frequencies, respectively.

intensity minima can be easily identified on the AGC voltage trace. The spectrum in the ionogram shows an upper cutoff structure with cutoff frequency near 0.6 MHz, well below the upper limit of the w-mode, f_H in this case being roughly equal to 0.5 f_N. The signal intensity sometimes exceeds -60 dBm (the saturating level of the sounder receiver) and appears to be spin-modulated deeper than estimated from the dipole antenna. Alouette 2 observations showed, however, no obvious dependence of w-mode emissions on antenna orientation (BARRINGTON *et al.*, 1971).

The latitudinal dependence of the plasma parameter f_N/f_H determined from resonance spikes on thirty three ionograms is given in Fig. 2, showing that data were obtained in rather high electron density region compared with those reported by BENSON and WONG (1987). There seems to be a maximum occurrence centered around 75 Inv. Lat., being consistent with Alouette-2 observations (BARRINGTON *et al.*, 1971) although the number of data points will be still insufficient.

Figure 3 shows the bandwidths of w-mode emissions as function of the ambient parameter, f_N/f_H. The upper cutoff frequency often exceeds half the local f_H for many cases, suggesting that the emissions come downward from the source region to the satellite. The cutoff frequencies are less than 0.1 MHz, the lowest frequency of the sounder for most cases. A few ionograms show the banded structures with lower cutoff frequency greater than 0.1 MHz. There seems to be no obvious dependence of the bandwidths on the plasma parameter, f_N/f_H. The spectral structure of these emissions appears to be similar to those observed by Ohzora satellite (MORIOKA and OYA, 1985; OYA *et al.*, 1985) and by ISIS-1 (BENSON and WONG, 1987). The

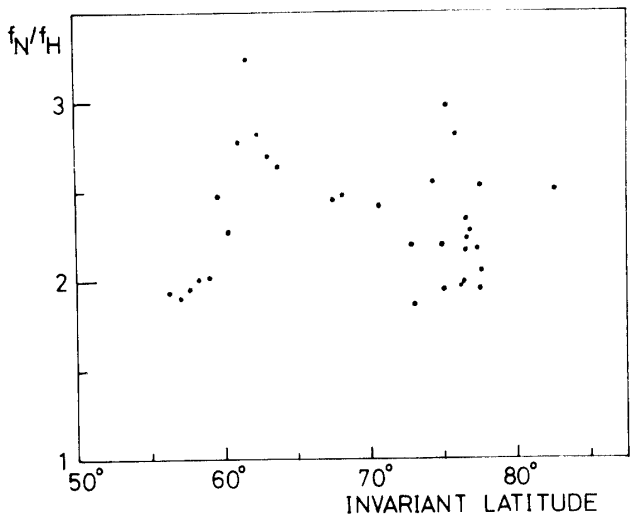

Fig. 2. Latitudinal dependence of plasma parameter f_N/f_H determined from resonance spikes on ionograms on which w-mode emissions can be seen.

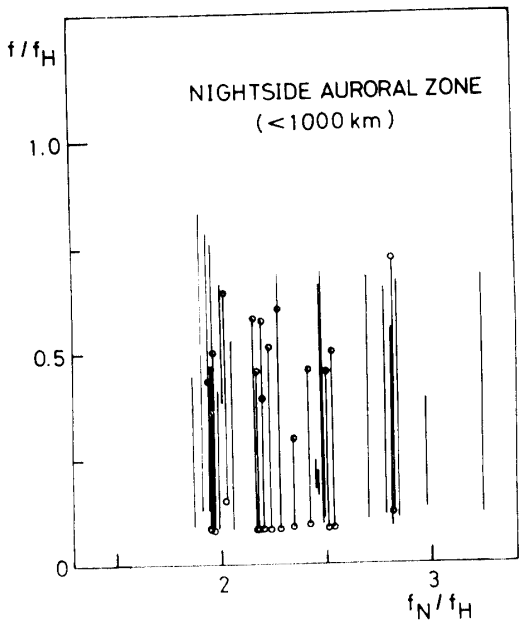

Fig. 3. Normalized frequency bandwidth of w-mode emissions versus local f_N/f_H. Vertical lines with circles at the tips correspond to intense emissions, whereas the vertical lines without circle to weak ones.

intensity seems, however, higher than that reported by BENSON and WONG (1987) and that of auroral LF hiss which is frequently observed in the dayside polar cusp. These spectra are evidently different from those of so called "type 2" emissions observed with $0.4<f/f_H<0.6$ in the polar E region (OYA *et al.*, 1980; MIYAOKA *et al.*, 1981).

2.2. *Direction of wave vector*

ISIS-1 is spin-stabilized at the spin rate of about 3 RPM with spin axis nearly perpendicular to the orbital plane (cartwheel-mode operation). In this case the spin modulation of received signal should be roughly 3 db because of long dipole antenna. The measured modulation of the emissions, however, often exceeds 10 db, indicating sources to be of a finite longitudinal spread. Under these situations the direction of wave vectors can be estimated from antenna orientation with respect to the geomagnetic field at the time when the intensity of the received emissions exhibits minimum under fixed frequency mode operation, using a technique developed by JAMES (1980). To do this reasonable assumptions are additionally needed that the orbital plane coincides with the magnetic meridian plane and the sources are located in the same plane.

Figure 4 shows a typical example of the variation of AGC voltage traces and the antenna orientation with respect to the geomagnetic field when w-mode emissions were observed on both the swept and fixed frequency ionograms. This example was recorded in the nightside auroral zone on the southbound pass of November 16, 1977, and is used for determination of directions of wave vector at receiving points. The arrows on the base lines of AGC traces in fixed frequency frames (F.F) are located at

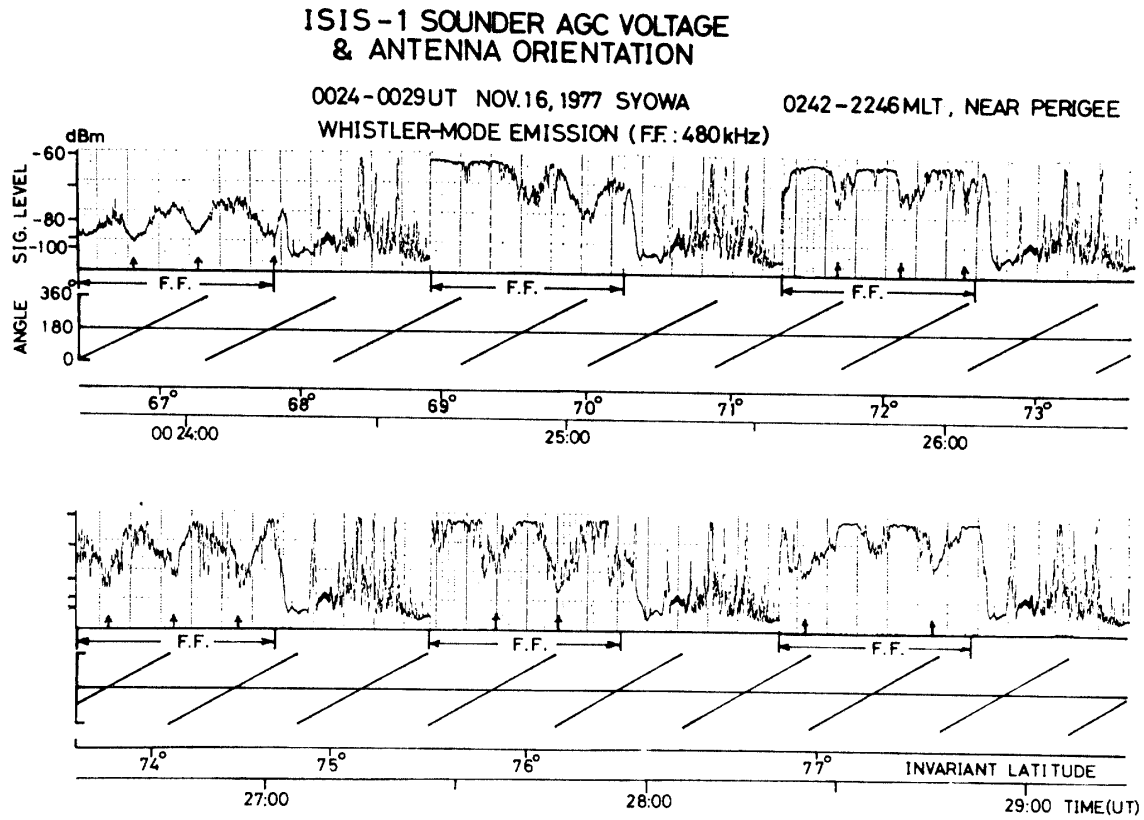

Fig. 4. Example of variations of AGC voltage traces and antenna orientation with respect to the geomagnetic field when w-mode emissions were seen on both swept and fixed frequency ionograms. The emissions were observed near perigee of the satellite in the nighttime auroral zone/polar cap on November 16, 1977. The portions labelled "F.F" correspond to the duration when the sounder was operated in the fixed frequency mode with 0.48 MHz.

minima of the AGC level estimated. In general, however, the fluctuation of AGC traces makes it difficult to locate the minimum points with a sufficient accuracy. The antenna orientation angle can be estimated with an accuracy of ± 1 degree, allowing for sampling rate of the magnetometer data. As seen in "F.F" portions the emissions exhibit remarkable increase in intensity around 68° Inv. Lat. and keep at high level up to Inv. Lat. higher than 77°. The orientation angle, δ at minimum points can be scaled with a reasonable accuracy; being $-10°$, $-13°$, $-6°$, and $-9°$, at 0025: 42, 0026: 02, 0028: 24 and 0028: 44 UT, respectively.

For a two-dimensional treatment the normal to the electric field plane (E-plane), $\boldsymbol{n}$ is estimated in magnetic meridional plane along with the ambient geomagnetic field $\boldsymbol{B}_0$ and wave vector $\boldsymbol{k}$ as shown in Fig. 5, where θ is an angle between $\boldsymbol{B}_0$ and $\boldsymbol{k}$, and ε an angle between $\boldsymbol{n}$ and $\boldsymbol{k}$. The angles θ and ε satisfy the general equation $\tan\varepsilon = (P-\mu^2)\tan\theta/P$, where $P=1-(f_N/f)^2$ and μ is the refractive index (JAMES, 1980). Also shown in the figure is the dependence of ε on θ as a function of wave frequency, f, for the designated f_N and f_H which are scaled on ionograms. From the geometry the angle δ must satisfy the relation, $\delta \leqq \delta_{max}$, where δ_{max} is an angle δ when ε equals the right angle, implying that θ gives the resonance cone angle θ_{res} and waves become electrostatic. For $f=0.48$ MHz the angle δ, which gives the angle between $\boldsymbol{B}_0$ and $\boldsymbol{n}$,

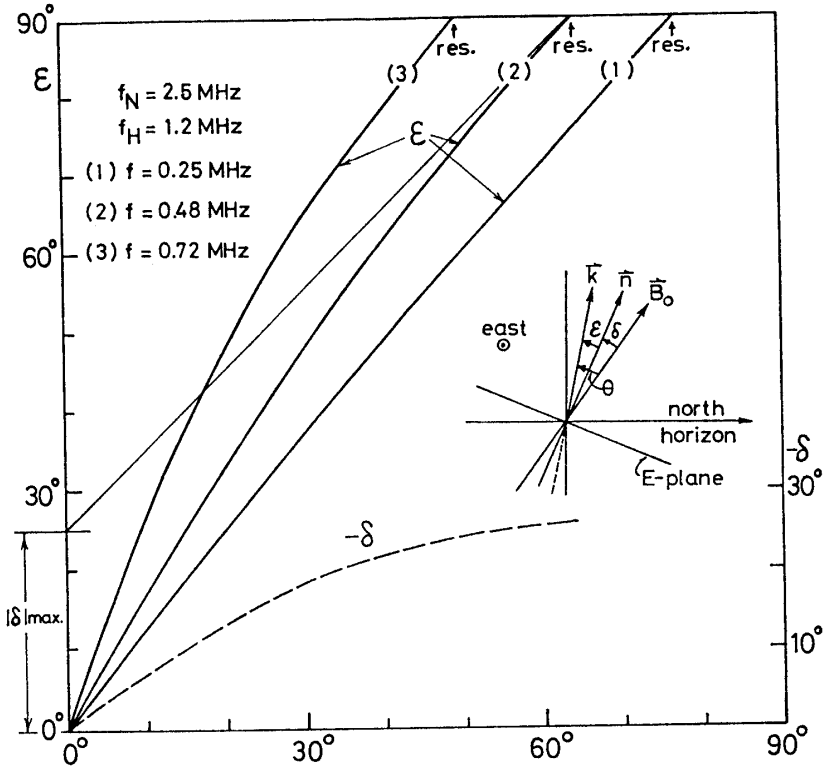

Fig. 5. Angle ε plotted as a function of angle θ. Three solid lines labelled (1) to (3) correspond to different frequencies specified in the figure. Also shown are the relation among three angles, ε, θ and δ to the direction of the geomagnetic field and the solution angle θ as a function of the angle δ.

is plotted as a function of θ by a graphical solution in the figure.

Using dashed curve the θ value are respectively determined to be about $-15°$, $-18°$, $-10°$ and $-13°$ for four values of δ previously scaled. This means that the wave vector lies close to the vertical, that is, off-angle less than five degrees, allowing for the dip angle of $\boldsymbol{B}_0$. Similar results are confirmed on the direction of wave vectors of w-mode emissions observed at low altitudes of the other three passes mentioned in the previous section. The low-altitude measurement of the wave vector directions at Syowa Station, Antarctica, revealed that the VLF hiss propagates downward with a large wave normal angle centered at about 75° to the geomagnetic field in the *E* and *F* regions (KIMURA *et al.*, 1981). The reflection at the bottom of the ionosphere, however, would prevent the hiss from being received on the ground. It is evident that small angle of the wave vector with respect to the vertical enable the emissions to penetrate into the ionosphere below the satellite and to be received with small attenuation on the ground. The simultaneous ground-based observations of VLF noises with frequency below about 30 kHz with telemetry reception from ISIS-1 indicated intense VLF hiss activities for all four passes, suggesting that wave vectors of the hiss lie within a few degrees of the vertical at the source region (SWIFT and KAN, 1975) and LF/MF emissions may be the high frequency part of the VLF hiss.

3. Propagation and Generation Mechanism

3.1. Ray tracing analysis

The ray tracing analysis was performed to examine the propagation of the emissions on the basis of wave vectors at the receiving points derived from spin minima data of fixed frequency AGC voltage obtained from the southbound pass of November 16, 1977. Rays were two-dimensionally traced backward from the receiving positions to the source regions using the three dimensional ray tracing program developed by JONES and STEPHENSON (1975), since the wave vector directions are determined two dimensionally. The electron density distribution of the model ionosphere/magnetosphere is constructed by giving latitudinal dependence of the electron density and temperature at a reference level of 1000 km so that the electron densities at an altitude of 600 km fit to values deduced from plasma resonance spikes on ionograms. The model also uses a simple dipole geomagnetic field and allows for plasmapause configuration (AIKYO *et al.*, 1972).

Figure 6 illustrates the 0.48 MHz ray paths starting at geomagnetic latitudes of 70° and 80° with an altitude of 600 km. Off-zenith angles χ_0 of the initial wave vectors are 4° and 1° for starting latitude of 70° and 5° and 2° for 80°, referring to the results mentioned in the preceding chapter. All rays go upward almost along the magnetic

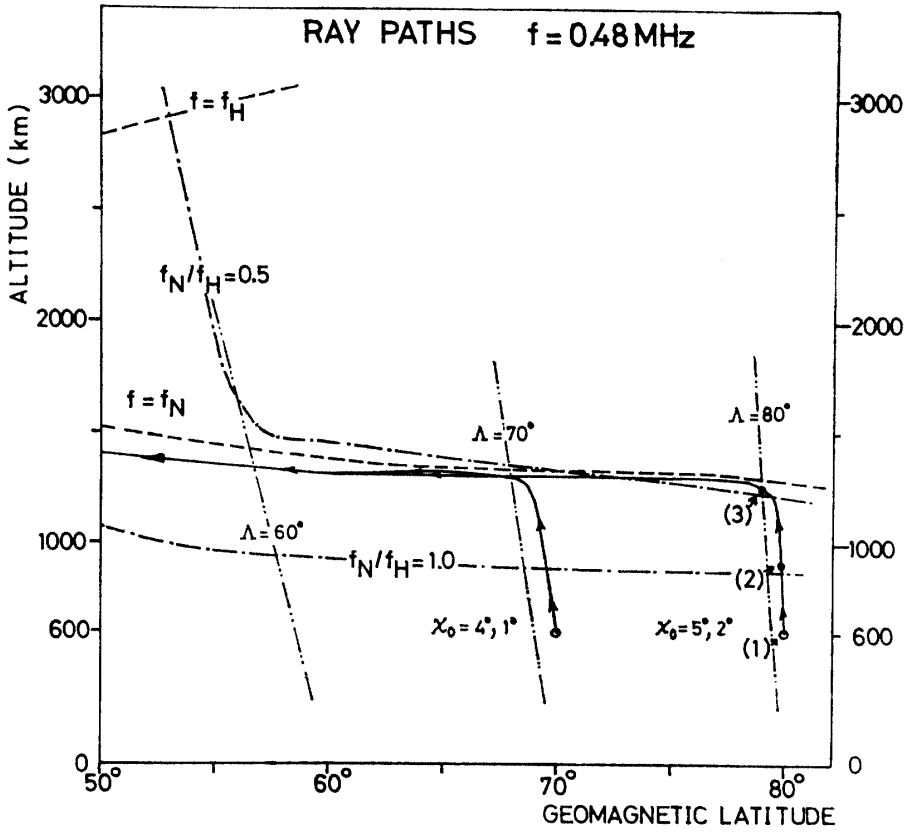

Fig. 6. Ray paths of a frequency of 0.48 MHz starting at geomagnetic latitudes of 70° and 80° with an altitude of 600 km in the model ionosphere/magnetosphere. Initial off-zenith angle χ_0 was determined from the angle θ solved using a graphical method described in Subsection 2.2.

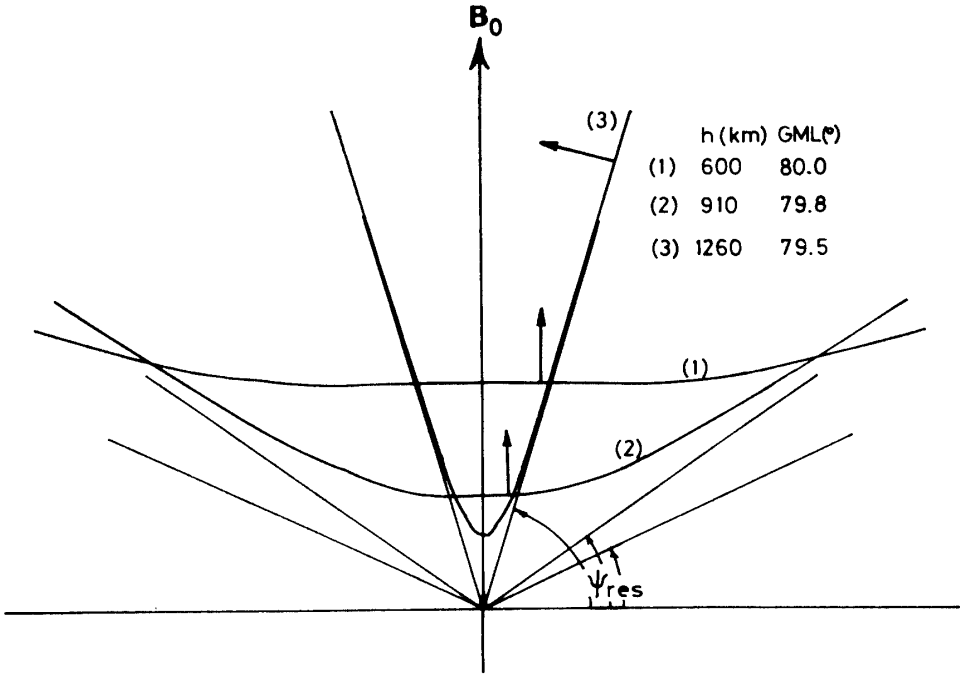

Fig. 7. Progressive change in the refractive index surfaces along a ray path starting at geomagnetic latitude of 80° shown in Fig. 6.

field lines until they approach to an altitude level where the wave frequency equals to f_N. The progressive change in the refractive index surface is shown in Fig. 7 where they are labelled successively (1), (2) and (3) corresponding to points on the ray starting at a geomagnetic latitude of 80°. The refractive index surfaces have resonance cones for wave frequency f and f_N and f_H concerned in this analysis. The values of f_N and f_H decrease as the rays proceed upward and the resonance angle ψ_{res} (complementary angle of resonance cone angle) tends to zero when f approaches to f_N because $\tan^2 \psi_{res}=(X-1)(Y^2-1)/(Y^2+X-1)$ where X and Y follow Ratcliff's notations. For this case the allowed wave vector directs almost parallel to the magnetic field and the direction of ray becomes almost perpendicular to the magnetic field, resulting in the wave being electrostatic. As a result the rays are bent abruptly at altitudes slightly lower than $f=f_N$ level. The rays proceed almost along a constant contour of electron density, $f=f_N$, meaning nearly horizontal propagation to the lower latitudes. Such propagation mode is identical with that of LF/MF hiss observed in the dayside cusp with ISIS-1 (JAMES, 1973). This result also suggests that sources must be located at lower latitudes than the latitudinal range of low altitude observations. From the viewpoint of propagations the source region must be below altitudes at which f_N equals to f for the frequency concerned because of f being less than the smaller of f_N and f_H, unless a mode conversion occurs between Z- and W-mode. As for 0.48 MHz rays in the assumed model the condition of $f=f_N=0.5f_H$ fortuitously satisfies when the rays proceed in the auroral zone keeping nearly horizontal propagation.

3.2. Generation mechanism

The spectra of the emissions sometimes exhibit banded structures with lower

cutoff frequency higher than 0.1 MHz, as described in Subsection 2.2. This suggests that the emissions are not necessarily higher frequency extension of the VLF hiss as often observed in the nightside auroral zone. Comparison of the intensities of W-mode emissions observed at high (BENSON, 1985) and low altitudes (BENSON and WONG, 1987) with ISIS-1 showed that the source region seems to be at altitudes below about 1500 km where f_N approximately equals to f_H. The spectra of the emissions have upper cutoff frequencies ranging from 0.75 to 0.4 MHz and lower cutoff frequencies below 0.1 MHz for most cases. Furthermore, the spectra provided by Hawkeye 1 observations show evidence of similarity of the generation mechanism between auroral kilometric radiation (AKR) and auroral hiss (GURNETT and GREEN, 1978). Thus it is worthwhile to reexamine the cyclotron maser instability (WU *et al.*, 1983) as a possible source of the W-mode emissions on the basis of some characteristics clarified by the present analysis.

As previously mentioned, the local plasma parameter f_N/f_H is roughly greater than two for the present case and thus the cyclotron resonance process is more efficient to generate w-mode emissions than Cerenkov resonance (SWIFT and KAN, 1975; MAGGS, 1978), as pointed out by BENSON and WONG (1987). WU *et al.* (1983) showed that a significant growth rate of w-mode emissions can be expected by cyclotron maser instability by auroral electron with upward loss cone. The emissions are strongly beamed downward along the geomagnetic field. The growth rate appears to be significant with the wave vectors within roughly 20° to the geomagnetic field for plasma parameters relevant to the auroral ionosphere, and its maximum occurs in a remarkably limited range of the normalized frequency f/f_H centered around 0.6. The dependence of the growth rate for parallel propagation, that is, beaming along the geomagnetic field upon the loss cone angle θ_c, the parameter f_N/f_H of local background plasma and the mean energy of reflected auroral electrons can be evaluated using the

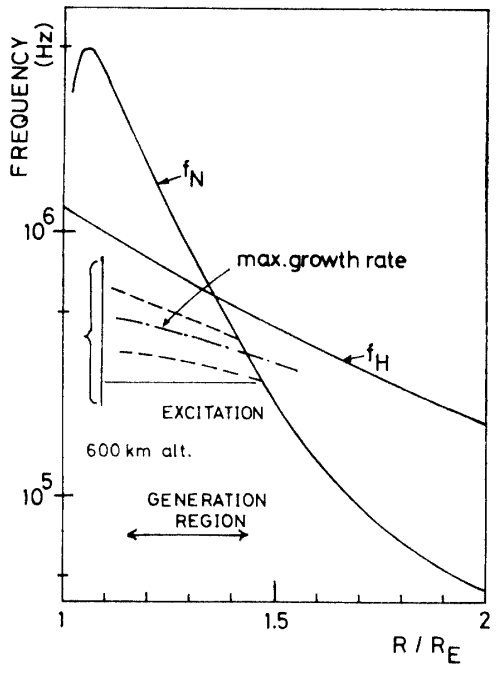

Fig. 8. Variation of f_N and f_H with normalized altitude R/R_E to interpret the spectral structure of high frequency portion of the emissions in terms of the cyclotron maser instability proposed by WU et al. (1983). A dash-dotted line shows variation of the frequency giving the maximum growth rate with altitude. Dashed lines indicate roughly the variation of the bandwidth.

eq. (17) in the paper of WU *et al.* (1983). The maximum growth rate increases monotonically with increasing energy, f_N/f_H and θ_c and the normalized frequency giving maximum growth rate decreases down to about 0.5. It must be noted that basic structure of the frequency spectra with narrow bandwidth from about 0.4 to 0.7 are scarcely affected by f_N/f_H, although the maximum value of the growth rate changes appreciably.

The observed spectra given in Fig. 3 can readily be interpreted in terms of such spectral form, by assuming that the sources of W-mode emissions distribute almost along the geomagnetic field so that the low frequency components received by the satellite are emitted at higher altitudes, as shown in Fig. 8, where the frequency giving the maximum growth rate is plotted along with the bandwidths as a function of altitude. At receiving point the upper cutoff frequency is roughly determined only by the local f_H, that is, about $0.6\,f_H$. It is evident that this mechanism can only be invoked to explain the higher frequency part of w-mode emissions because the significant growth rate requires that the value of f_N/f_H must be about unity or greater, and the frequency of w-mode waves is bounded by the higher limit of the smaller of f_N and f_H, as can be seen in Fig. 8. For lower frequency part of the emissions the Cerenkov resonance process is a more possible candidate of generation mechanism because the significant growth rate can be expected at all frequencies between the lower hybrid resonance frequency and f_N for low electron density condition (SWIFT and KAN, 1975; MAGGS, 1978).

At the source region the wave vectors of the emissions direct downward nearly along the geomagnetic field, satisfying the propagation condition at altitudes where the wave frequency almost equals to f_N, resulting in nearly horizontal propagation. Recent DE-1 and 2 observations of the precipitating electrons with loss cones show the latitudinal distribution with the maximum intensity near 66°–69° Inv. Lat. (LIN *et al.*, 1985) being consistent with the fact that the emissions are observed at higher latitudes at lower altitudes.

4. Concluding Remarks

Various types of plasma wave emissions can be seen on the ISIS-1 topside sounder ionograms obtained over the nightside auroral zone and the polar cap. Among the emissions the broadband whistler-mode emissions observed at low altitudes near the perigee (~ 600 km) over the Antarctic region are examined in detail concerning frequency spectral characteristics and propagation using ray tracing technique. The emissions observed at low altitudes by ISIS-1 are characterized by spectra with a sharp upper frequency cutoff ranging from 0.75 down to $0.4\,f_H$ and with a lower frequency cutoff less than 0.1 MHz (the lowest frequency limit of the sounder) for many cases of intense emissions.

On the basis of the spin-modulated signals on the fixed frequency ionograms obtained when the satellite was in the cartwheel-mode operation, the antenna orientation at the instant of minimum emissions was determined for deriving the direction of arrival of emissions, using the local plasma parameters deduced from the swept-frequency ionograms. The obtained direction of the propagation vector appears to

be approximately vertical, implying that the emissions come downward from sources above the satellite. A simple ray tracing was performed to locate the source region for the emissions using a plausible model ionosphere/magnetosphere, and it was shown that some characteristics, especially on the high frequency components of the emissions, can be well interpreted in terms of the cyclotron maser instability driven by precipitating auroral electrons with upward loss-cones as a most possible source mechanism, which is most effective process at low altitudes ($f_N > f_H$) in the nighttime auroral zone.

Acknowledgments

The authors thank Dr. J. H. WHITTEKER and Mr. J .D. R. BOULDING, Communications Research Centre (CRC), Department of Communications, Canada, NASA, U. S. A. and ISIS Working Group for their supports to the ISIS topside sounder observations at Syowa Station, Antarctica. The authors are also grateful to the members of the wintering parties of the 17th–22nd Japanese Antarctic Research Expeditions at Syowa Station for their collaboration in ISIS data acquisition for the present analysis. The kind generosity of CRC staff, especially Dr. H. G. JAMES, to offer invaluable information for interpretation of the ISIS magnetometer data is greatly appreciated.

References

AIKYO, K., ONDOH, T. and NAGAYAMA, M. (1972): Nonducted whistlers observed in the plasmasphere. J. Radio Res. Labs., **19**, 151–174.

AIKYO, K., ONDOH, T., NISHIZAKI, R., MARUYAMA, T., IGI, S., NAGAYAMA, M., YABUUMA, H., IDE, T. and HIRASAWA, T. (1982): Spectral characteristics of radio noise at low and medium frequencies in the Antarctic topside ionosphere. Mem. Natl Inst. Polar Res., Spec. Issue, **22**, 82–93.

BARRINGTON, R. E., HARTZ, T. R. and HARVEY, R. W. (1971): Diurnal distribution of ELF, VLF, and LF noise at high latitudes as observed by Alouette 2. J. Geophys. Res., **76**, 5278–5291.

BENSON, R. F. (1985): Auroral kilometric radiation; Wave modes, harmonics, and source region electron density structure. J. Geophys. Res., **90**, 2753–2784.

BENSON, R. F. and WONG, H. K. (1987): Low-altitude ISIS 1 observations of auroral radio emissions and their significance to the cyclotron maser instability. J. Geophys. Res., **92**, 1218–1230.

GURNETT, D. A. and GREEN, J. L. (1978): On the polarization and origin of auroral kilometric radiation. J. Geophys. Res., **83**, 689–696.

JAMES, H. G. (1973): Whistler-mode hiss at low and medium frequencies in the dayside-cusp ionosphere. J. Geophys. Res., **78**, 4578–4599.

JAMES, H. G. (1980): Direction-of-arrival measurements of auroral kilometric radiation and associated ELF data from ISIS 1. J. Geophys. Res., **85**, 3367–3375.

JONES, R. M. and STEPHENSON, J. J. (1975): A versatile three-dimensional ray tracing computer program for radio waves in the ionosphere. OT Rept. **75–76**, Office of Telecom. U. S. Dept. Commerce.

KIMURA, I., MATSUO, T., TSURUDA, K. and YAMAGISHI, H. (1981): Measurements of the directions of propagation vector and Poynting flux of auroral hiss by means of the S-310JA-5 rocket. Mem. Natl Inst. Polar Res., Spec. Issue, **18**, 439–452.

LIN, C. S., BARFIELD, J. N., BURCH, J. L. and WINNINGHAM, J. D. (1985): Near-conjugate observations of inverted-V electron precipitation using DE 1 and 2. J. Geophys. Res., **90**, 1669–1681.

MAGGS, J. E. (1978): Electrostatic noise generated by the auroral electron beam. J. Geophys. Res., **83**, 3173–3188.

MIYAOKA, H., OYA, H. and MIYATAKE, S. (1981): Observations of MF-HF plasma wave emissions in the polar ionosphere using the Antarctic rockets S-310JA-4 and S-310JA-6. Mem. Natl Inst. Polar Res., Spec. Issue, **18**, 462–490.

MORIOKA, A. and OYA, H. (1985): Emissions of plasma waves from VLF to LF ranges in the magnetic polar regions—New evidences obtained from the data of the Ohzora (EXOS-C) satellite. J. Geomagn. Geoelectr., **37**, 263–284.

MULDREW, D. B. (1970): Preliminary results of ISIS 1 concerning electron-density variations, ionospheric resonances and Cerenkov radiation. Space Res., **10**, 786–794.

OYA, H., MIYAOKA, H. and MIYATAKE, S. (1980): Nankyoku roketto S-210JA-21-gôki ni yoru kôshûha purazuma hadô supekutoru no kansoku (Observation of HF plasma wave spectrum at ionospheric level using sounding rocket S-210JA-21 in Antarctica). Nankyoku Shiryô (Antarct. Rec.), **69**, 37–51.

OYA, H., MORIOKA, A. and OBARA, T. (1985): Leaked AKR and terrestrial hectometric radiations discovered by the plasma wave and planetary plasma sounder experiments on board the Ohzora (EXOS-C) satellite-instrumentation and observation results of plasma wave phenomena. J. Geomagn. Geoelectr., **37**, 237–262.

SWIFT, D. W. and KAN, J. R. (1975): A theory of auroral hiss and implications on the origin of auroral electrons. J. Geophys. Res., **80**, 985–992.

WU, C. S., DILLENBURG, D., ZIEBELL, L. F. and FREUND, H. P. (1983): Excitation of whistler waves by reflected auroral electrons. Planet. Space Sci., **31**, 499–507.

(Received June 1, 1987; Revised manuscript received July 31, 1987)